Construction of shell-like carbon superstructures through anisotropically oriented self-assembly for distinct electromagnetic wave absorption

Xiao Li[a], Haowei Zhou[a], Jinlin Zhang[a], Xinyue Zhang[b], Man Li[a], Jieyan Zhang[a], Moustafa Adel Darwish[c], Tao Zhou[d], Shi-Kuan Sun[e], Lei Xie[b,], Di Zhou[a,]**

[a]Multifunctional Materials and Structures, Key Laboratory of the Ministry of Education & International Center for Dielectric Research, School of Electronic Science and Engineering, Xi'an Jiaotong University, Xi'an, 710049, PR China. E-mail: zhoudi1220@xjtu.edu.cn

[b]The Key Laboratory of Biomedical Information Engineering of Ministry of Education, School of Life Science and Technology, Xi'an Jiaotong University, Xi'an, 710049, PR China. E-mail: leixie@xjtu.edu.cn

[c]Physics Department, Faculty of Science, Tanta University, Al-Geish st., Tanta 31527, Egypt.

[d]School of Electronic and Information Engineering, Hangzhou Dianzi University, Hangzhou, 310018, PR China.

[e]School of Material Science and Energy Engineering, Foshan University, Foshan, Guangdong, 528000, PR China.

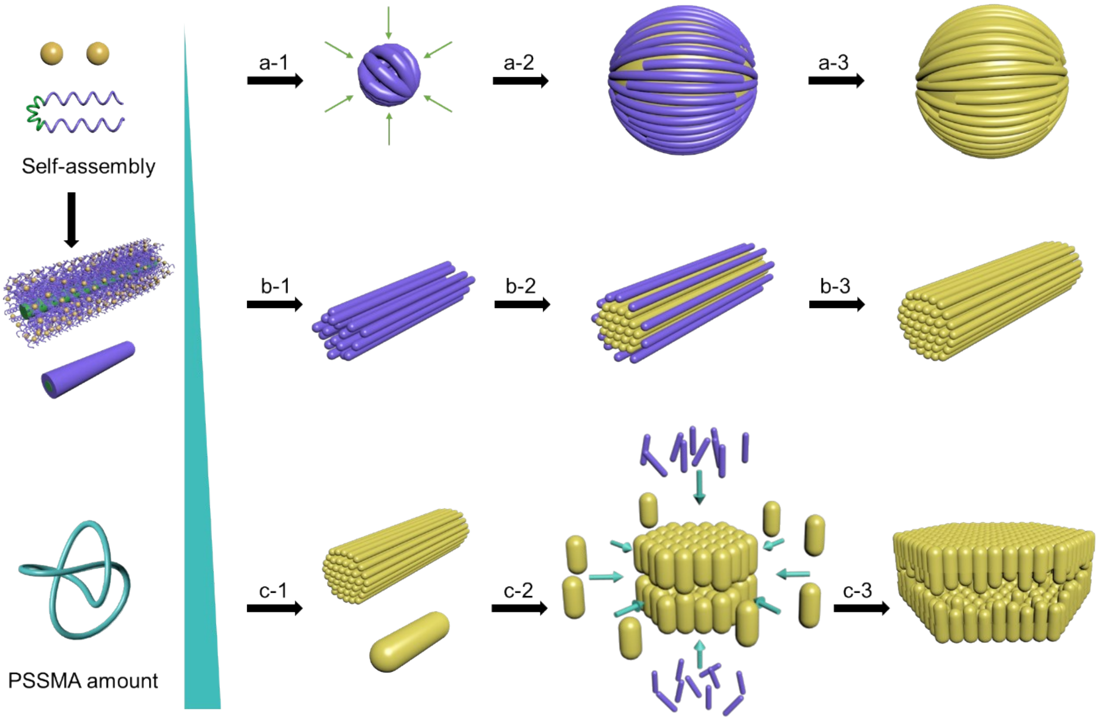

Figure S1. The formation mechanism of various carbon materials with different PSSMA amount. (a) sphere-like carbon material without PSSMA, (b) rod-like carbon material with 100 mg of PSSMA, and (c) shell-like carbon superstructure with 150 mg of PSSMA.

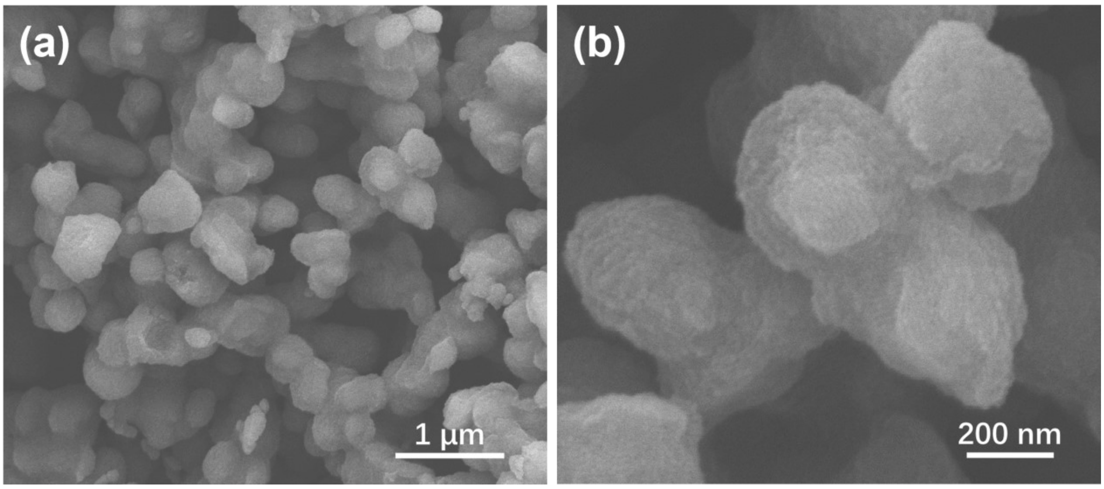

Figure S2. SEM images of sphere-like carbon materials.

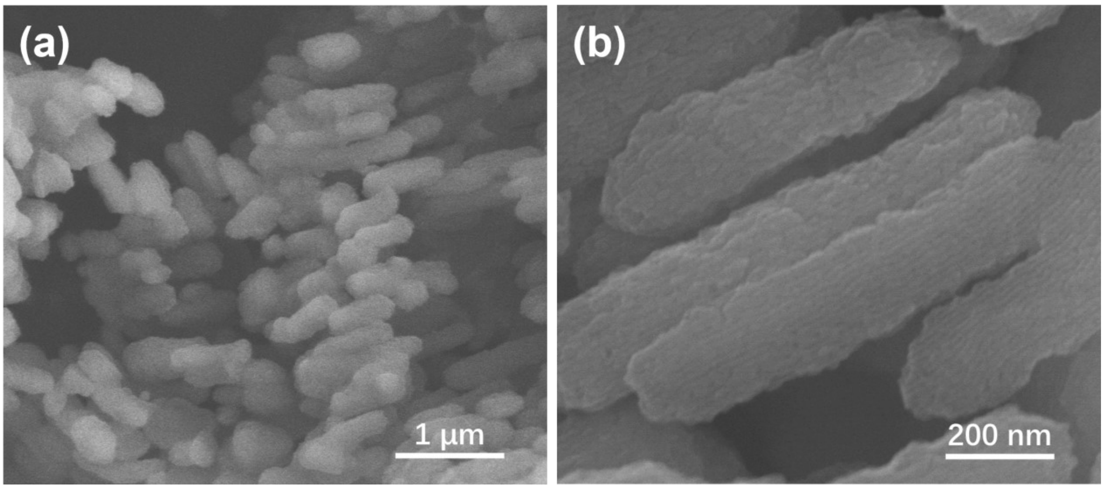

Figure S3. SEM images of rod-like carbon materials.

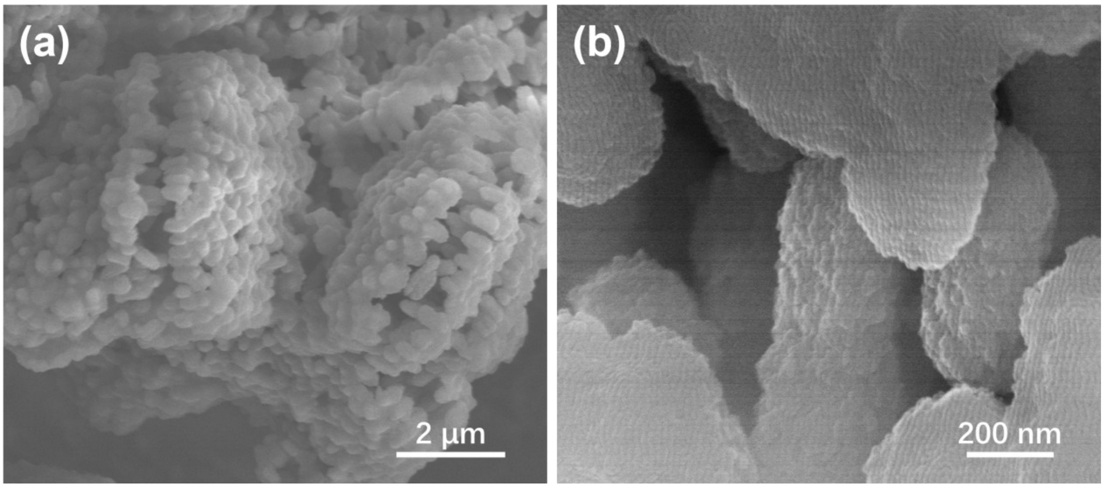

Figure S4. SEM images of shell-like carbon superstructures.

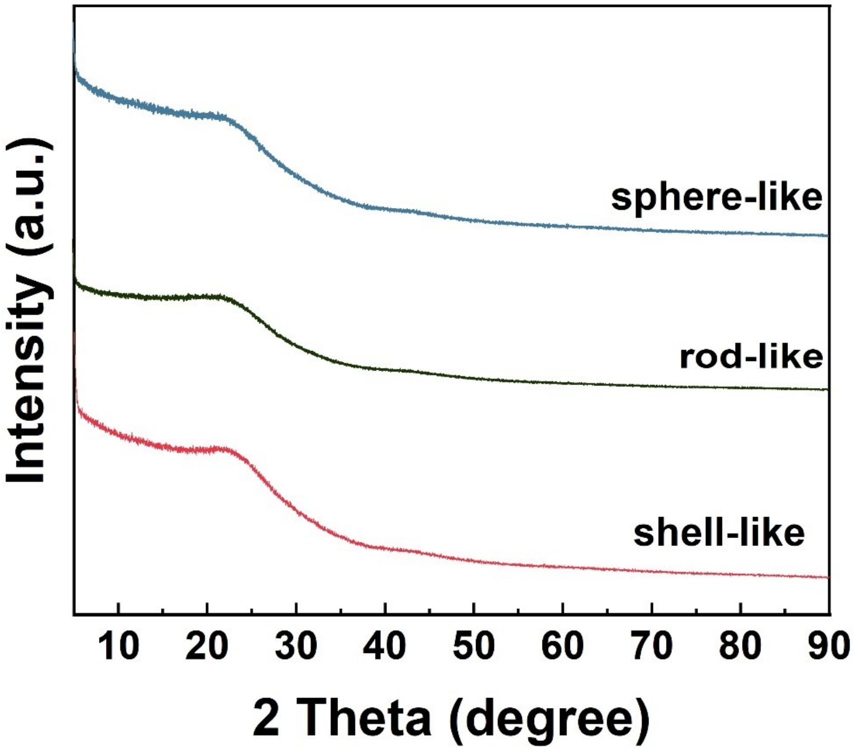

Figure S5. XRD patterns of three samples.

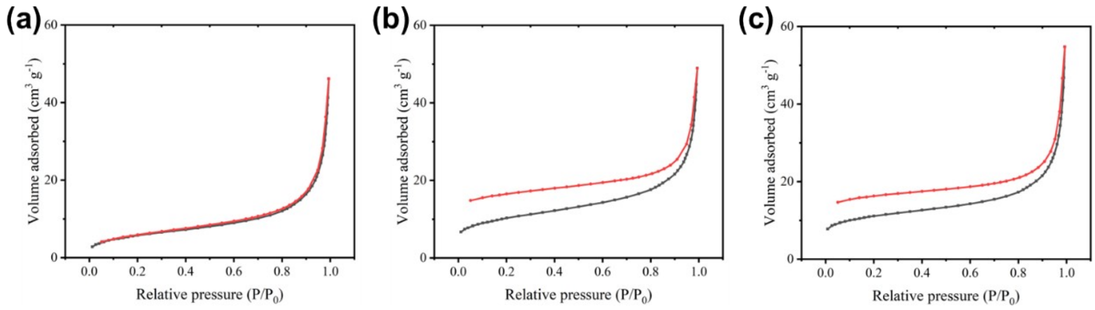

Figure S6. Nitrogen adsorption desorption isotherms of (a) sphere-like, (b) rod-like, and (c) shell-like carbon superstructures.

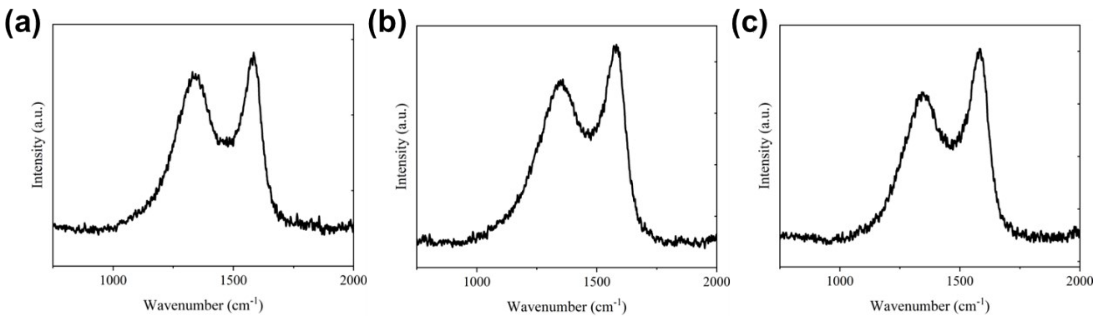

Figure S7. Raman spectra of (a) sphere-like, (b) rod-like, and (c) shell-like carbon superstructures.

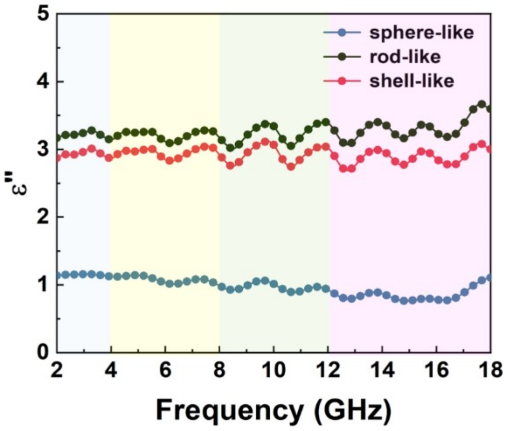

Figure S8. Imaginary part of the permittivity vs frequency of sphere-like, rod-like and shell-like carbon superstructures.

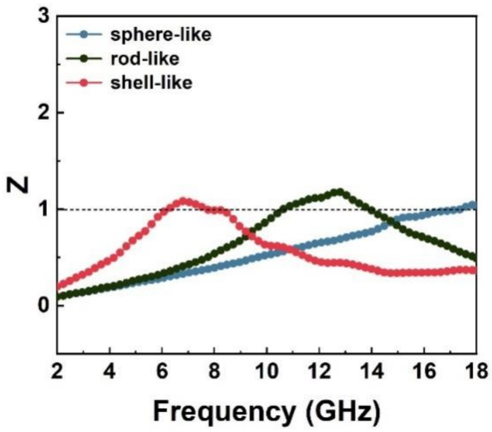

Figure S9. Z values vs frequency of three samples at the thicknesses corresponding to their respective strongest reflection loss values.

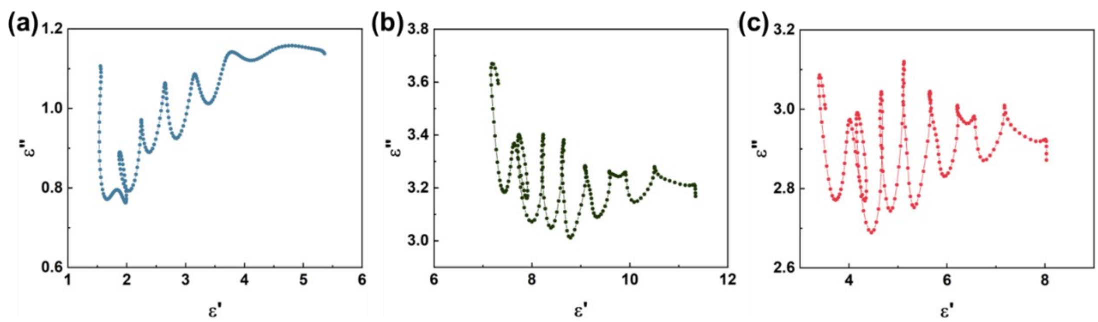

Figure S10. Cole-Cole curves vs frequency of (a) sphere-like, (b) rod-like, and (c) shell-like carbon superstructures.

Table S1. Microwave absorption properties of carbon materials have been reported.

Absorber	Maximum RL（dB）	Matching frequency（GHz）	Maximum EAB（GHz）	Matching thickness(mm)	Ref

N-doped carbon microsphere composites with concavo-convex surface	-46.8	10.4	3.7	2.7	S1
Biomass hierarchical porous carbon	-47.463	9.796	3.402	2.8	S2
hollow carbon cubes	-38.0	—	1.1	4	S3
porous carbon hollow nanoboxes	-30.46	15.68	5.44	2.2	S4
mushroom cap-shaped porous carbon particles	-42.40	14.86	4.37	1.6	S5
Multi-shell hollow porous carbon nanoparticles	-18.13	14.66	5.17	1.6	S6
Shaddock Peel-Based Carbon	-29.50	—	2.44	2.5	S7
three-dimensional cross-linked carbon fiber	-44.44	—	3.64	1.17	S8

References

[S1] Wang, J.; Ren, J.; Li, Q.; Liu, Y.; Zhang, Q.; Zhang, B. Synthesis and Microwave Absorbing

Properties of N-Doped Carbon Microsphere Composites with Concavo-Convex Surface. *Carbon* **2021**, *184*, 195-206.
[S2] Wu, Z.; Meng, Z.; Yao, C.; Deng, Y.; Zhang, G.; Wang, Y. Rice Husk Derived Hierarchical Porous Carbon with Lightweight and Efficient Microwave Absorption. *Materials Chemistry and Physics* **2022**, *275*.
[S3] Yuan, C.; Wu, W.-W.; Liu, Y.; Wang, Z.; Wang, Y.; Han, L.-L.; Zhou, Q.; Liu, J.-Q.; Liu, P. High Yield Hollow Carbon Cubes with Excellent Microwave Absorption Property at a Low Loading Ratio. *Carbon* **2022**, *195*, 101-111.
[S4] Wei, S.; Shi, Z.; Wei, W.; Wang, H.; Dastan, D.; Huang, M.; Shi, J.; Chen, S. Facile Preparation of Ultralight Porous Carbon Hollow Nanoboxes for Electromagnetic Wave Absorption. *Ceramics International* **2021**, *47* (19), 28014-28020.
[S5] Yang, W.; Yang, X.; Hu, J.; Liu, D.; Dong, Y.; Zhu, Y.; Fu, Y. Mushroom Cap-Shaped Porous Carbon Particles with Excellent Microwave Absorption Properties. *Applied Surface Science* **2021**, *564*.
[S6] Tao, J.; Zhou, J.; Yao, Z.; Jiao, Z.; Wei, B.; Tan, R.; Li, Z. Multi-Shell Hollow Porous Carbon Nanoparticles with Excellent Microwave Absorption Properties. *Carbon* **2021**, *172*, 542-555.
[S7] Gu, W.; Sheng, J.; Huang, Q.; Wang, G.; Chen, J.; Ji, G. Environmentally Friendly and Multifunctional Shaddock Peel-Based Carbon Aerogel for Thermal-Insulation and Microwave Absorption. *Nano-Micro Letters* **2021**, *13* (1), 10201-10214.
[S8] Dai, B.; Li, J.; Liu, X.; Wang, N.; Dai, Y.; Qi, Y. Multiple Synergistic Losses in the Absorption of Electromagnetic Waves by Three-Dimensional Cross-Linked Carbon Fiber. *Carbon* **2022**, 195, 308-318.